Gut, 1991, 32, 858–865

Different types of peroxisomes in human duodenal epithelium

F Roels, M Espeel, M Pauwels, D De Craemer, H J A Egberts, P van der Spek

Abstract

Peroxisomes are ubiquitous organelles containing enzyme sequences for β oxidation of fatty acids, synthesis of bile acids, and ether phospholipids. In the inherited peroxisomal diseases one or more enzymes are deficient in hepatic, renal, and fibroblast peroxisomes. We have examined peroxisomes by light and electron microscopy in 29 duodenal biopsy specimens (21 with normal mucosa) after staining for catalase activity, a marker enzyme. Peroxisomes were most numerous in the apices of the nucleus and at the villus base. Two types were distinguished: rounded to oval forms with a median lesser diameter of 0·23–0·31 μm, and tubular, vermiform organelles 0·1 μm thick and up to 3 μm long. Both types coexist in most patients. Tilting of sections and examination of semithin sections at 120 kV did not show connections between individual organelles. By morphometry, volume density was at least 0·45–0·62% of cellular volume, compared to 1·05% in human liver. In contrast, in four out of five individuals surface density of the peroxisomal membrane was 1·4–2·3 times higher than in control livers; this is expected to favour the exchange of metabolites. We suggest that intestinal peroxisomes contribute substantially to the breakdown of very long chain fatty acids.

Peroxisomes are cell organelles involved in the breakdown of very long chain fatty acids, synthesis of bile acids and plasmalogens (ether phospholipids), and metabolism of glyoxylate avoiding formation of oxalate. Congenital deficiencies of these enzymes lead to severe diseases such as the cerebrohepatorenal syndrome of Zellweger, adrenoleucodystrophy (neonatal, juvenile, and adult forms), infantile Refsum's disease (phytanic acid storage), chondrodysplasia punctata (rhizomelic as well as Conradi-Hünermann forms), and primary hyperoxaluria type I.[1–8] Most studies on peroxisomes have been performed in liver and most recently on cultured fibroblasts. In intestinal epithelium the first studies were performed in the guinea pig[9 10] and in one case in human jejunum.[11] In human duodenum (15 samples) the presence of peroxisomes was shown by tissue fractionation by Peters.[12]

We have visualised peroxisomes for light and electron microscopy in 29 routine duodenal biopsy specimens from adults by staining for the marker enzyme catalase. We describe different forms and their distribution in the cell and over the villus. After our first results were reported,[13 14] normal looking[1] and altered[15 16] peroxisomes were found in the duodenum of children with neonatal adrenoleucodystrophy and the Zellweger syndrome.

Methods

Among biopsy specimens taken for diagnostic purposes, 21 were selected because the mucosa at the angle of Treitz was macroscopically and microscopically normal. In addition, eight pathological cases were examined but detailed results are not reported here. The diagnoses in the 29 patients are given in Table I. There were 15 men and 14 women, age range 20–81 years, mean (SD) 55 (17·6) years.

The tissue was fixed at room temperature in 4% formaldehyde + 1% $CaCl_2$ buffered by 0·12 M cacodylate over 24 hours.[17] After a brief rinse in buffered calcium chloride fragments were cut with a razor blade under a binocular microscope parallel with the villus axis, and incubated for catalase activity with diaminobenzidine at pH 9·4 and 45°C or pH 10·5 at 22°C.[3 18] Cytochemical controls consisted of incubation after enzyme inactivation at 75°C, and staining of unfixed fragments at pH 7·3 for peroxidase excluding catalase.[19] Postosmication was performed in the presence of potassium ferricyanide.[3 18] Epon sections 1 and 4 μm were examined in phase contrast. For electron microscopy, 600 Å sections were cut parallel to the villus axis and counterstained with lead only. In addition, 0·4–1 μm sections were examined at 100 or 120 kV.

Peroxisomes were compared at four levels of a villus (tip, stem, base, and crypt) from the same patient; this was done in five patients.

MORPHOMETRY

Electron micrographs were taken at random over the entire epithelial cell between brush border

TABLE I *Diagnosis in 29 patients*

Normal duodenal mucosa at angle of Treitz:	21
Gastritis	6
Corticosteroid treatment, gastritis	1
Gastric tumour, gastritis	1
Cirrhosis, diabetes, gastritis	1
Healed gastric ulcer	1
Gastritis, renal failure	1
Gastric ulcer	1
Oesophageal bleeding	1
Reflux oesophagitis	1
Bulbitis	2
Duodenal ulcer	2
Duodenal ulcer, oesophagitis	1
Healed duodenal ulcer	1
Duodenal ulcer, multiple sclerosis	1
Duodenitis:	6
No other pathology	3
Gastrectomy B I	1
Scleroderma, oesophagitis	1
Alcoholic cirrhosis, old ulcus bulbi	1
Subtotal gastrectomy B II, blind loop	1
Coeliac disease with severe atrophy	1

Human Anatomy
F Roels
M Espeel
M Pauwels
D De Craemer

and Department of Gastroenterology, Academic Hospital, Vrije Universiteit, Brussels, Belgium
P van der Spek

Department of Veterinary Pathology, State University of Utrecht, The Netherlands
H J A Egberts

Correspondence to:
Professor Frank Roels, Human Anatomy, Laarbeeklaan 103, 1090 Brussels, Belgium.

Accepted for publication 10 September 1990

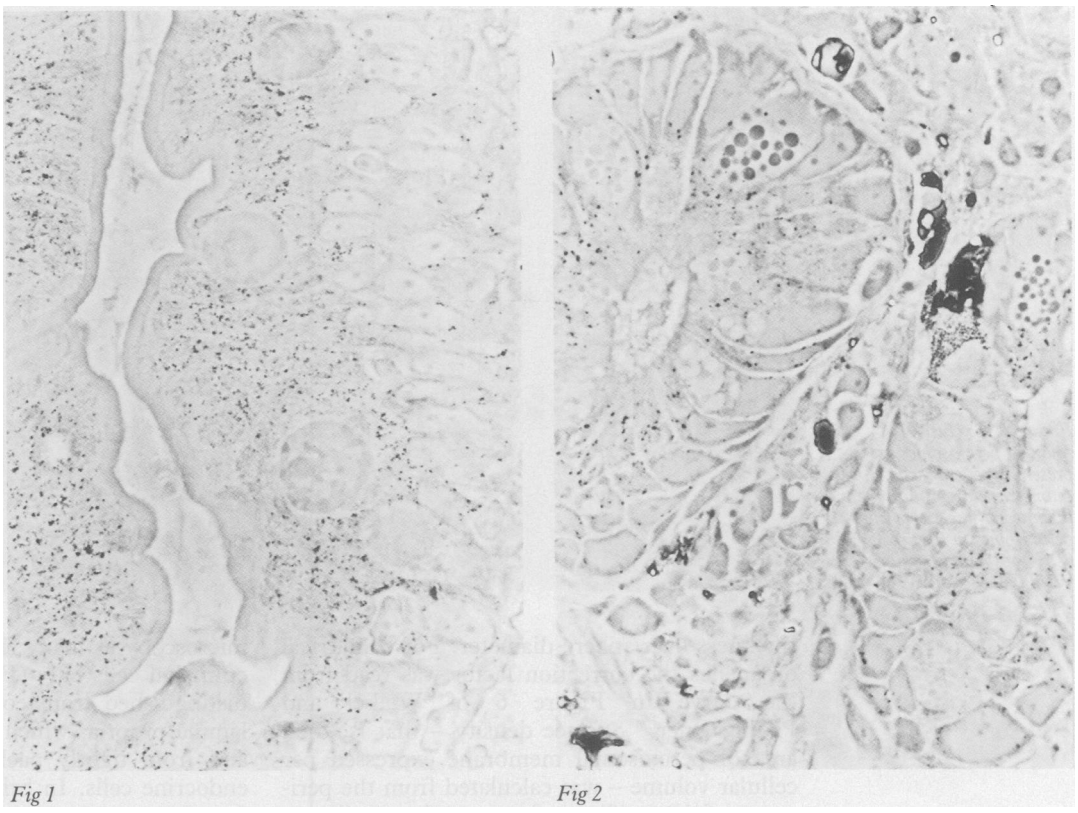

Figures 1 and 2: In the light microscope peroxisomes are visualised as tiny black granules. They are most abundant at the villus base and apex of the nucleus (Fig 1). In the crypt cells they are well stained but there are few (Fig 2). Paneth cells can be recognised. 1 μm Epon sections, phase contrast. (Original magnification ×950.)

and basal membrane; this was done in five patients. Peroxisomes were measured by means of a graphic tablet (Ibas I, Kontron) at a final magnification of approximately 35 000, which was calibrated with a grating replica in each series of photographs. In addition to size, the formfactor area $.4\pi/\text{perimeter}^2$ (perfect circle=1) was computed. The width (thickness, lesser diameter) of elongated structures was estimated by area/long diameter (D-ellips A). If curved tubules are measured D-ellips A is shorter than the true length and width is overestimated, while in a circular profile the calculated width is 1·274 times smaller than the true diameter. For these reasons size was also measured manually in a limited sample. Volume density was calculated as total peroxisomal area over reference cellular area including the nucleus, with or without correction for sections of finite thickness[20]: for spherical organelles the corrected volume density=area of profiles/area of reference×2/2+ 3×relative section thickness – that is, section

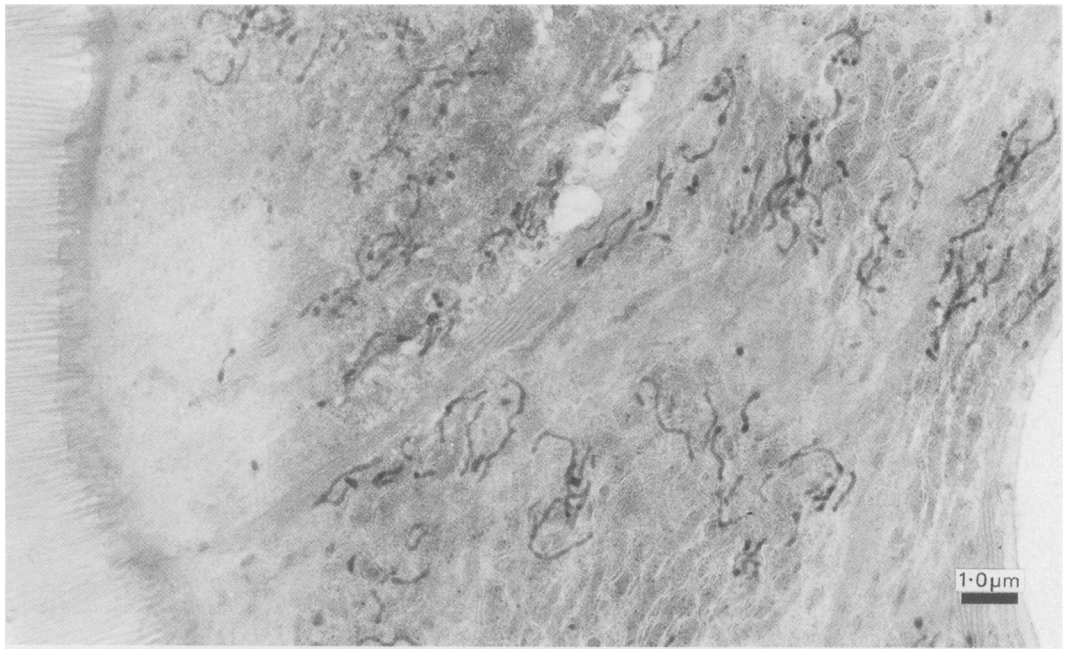

Figure 3: Worm like peroxisomes as observed in a semithin (0·6 μm) section by electron microscopy at 120 kV. Their orientation is random. No spherical organelles are identified in these cells. Compare with Figure 4 (×7600).

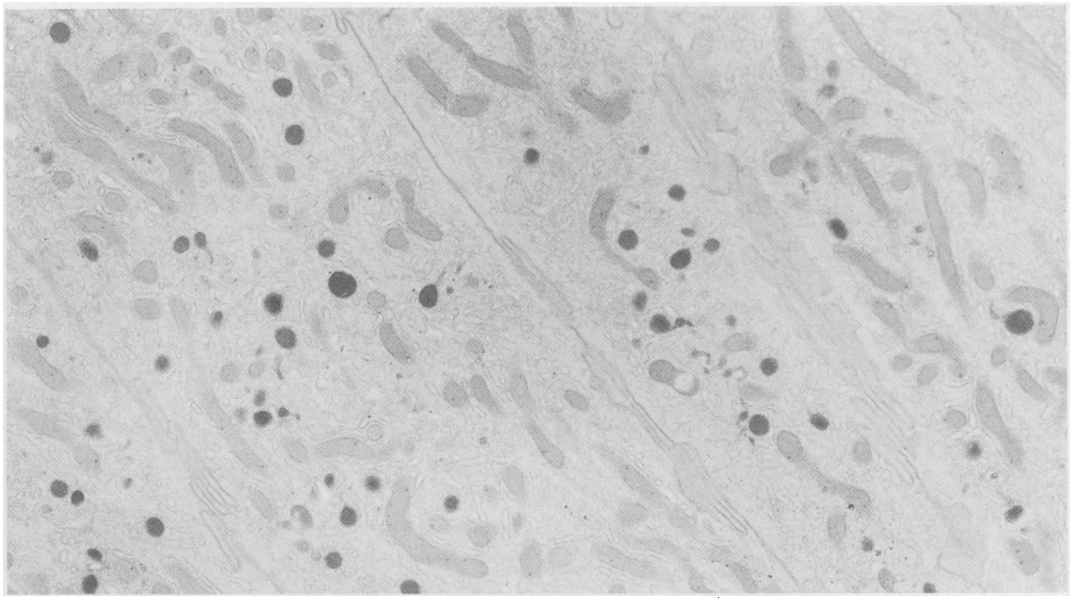

Figure 4: Exclusively rounded peroxisomes are present in several cells. Their diameter is larger than the thickness of the worm like peroxisomes in Figure 3. (Original magnification ×7600.)

thickness over sphere diameter. For cylindrical organelles the correction factor was read from the curve in Figure 6 of Weibel and Paumgartner.[20] Surface density – that is, total area of peroxisomal membrane expressed per cellular volume – was calculated from the perimeter of the profiles and corrected according to Weibel and Paumgartner.[20] Surface density was also determined in six human livers which were microscopically normal.

Results

LIGHT MICROSCOPY

Peroxisomes were visualised by phase contrast microscopy as many tiny black granules in the epithelial cells only (Figs 1 and 2). They were distinguished from eosinophil granules in the lamina propria (which are very large and oval) and from tightly packed granules in solitary endocrine cells. In bright field microscopy the peroxisomes were less easily seen. They were not detectable after both control incubations.

The intracellular distribution was not homogeneous; peroxisomes were limited to the region apical of the nucleus in two thirds of the samples; a few further granules were seen basal to the nucleus in one third (Fig 1). They were most abundant and well stained at the villus base. In the crypts staining was strong but there were fewer granules (Fig 2). They were occasionally seen in

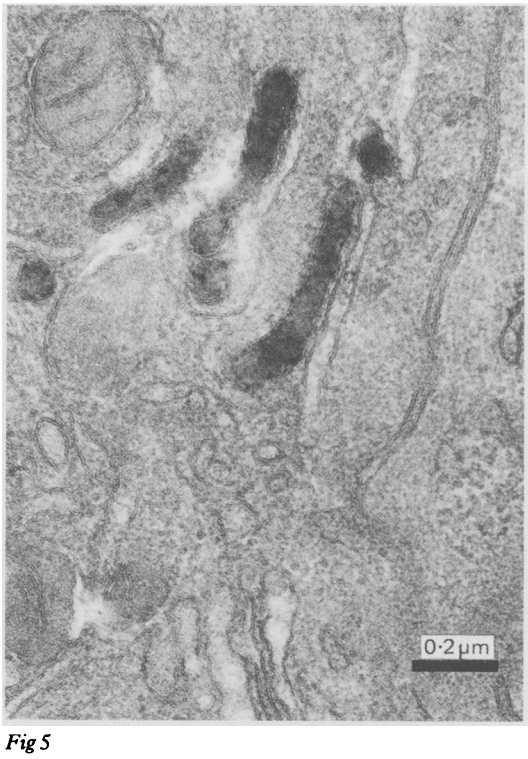

Fig 5

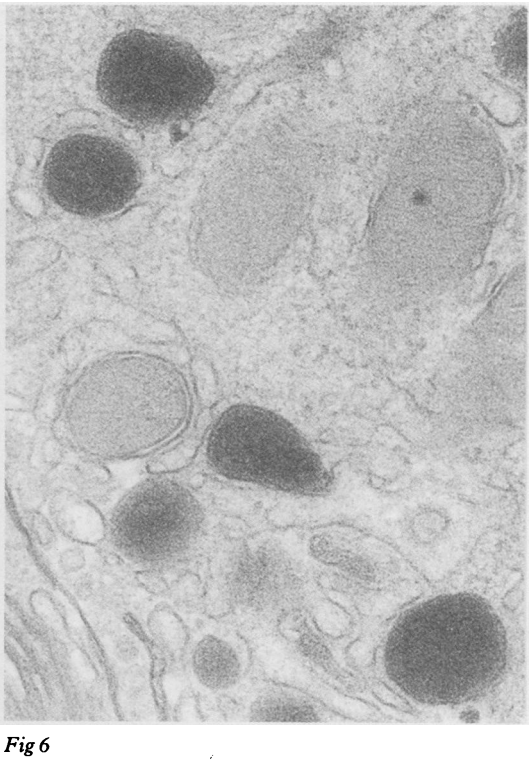

Fig 6

Figures 5 and 6: Tubular and rounded profiles at high magnification. Differences in thickness are evident. Endoplasmic reticulum cisternae are close to peroxisomes but unreactive for catalase; they are still narrower than the tubular peroxisomes. Part of a Golgi apparatus is seen in both images. (Original magnification × 51 000.)

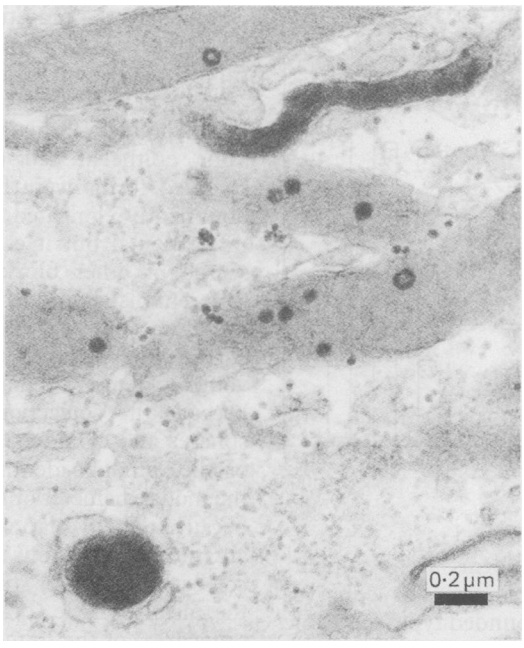

Figure 7: A worm like and rounded peroxisome in the same cell. Note difference in lesser diameter. Both are associated with smooth endoplasmic reticulum cisternae. (Original magnification ×34 000.)

a mitotic cell. Near and at the villus tip the catalase reaction was weak or even absent.

No obvious differences between patients were observed except in the biopsy specimen taken from the blind loop after gastrectomy and in the low epithelium of the patient with coeliac disease. In both the catalase reaction was weak and the number of granules few.

ELECTRON MICROSCOPY

Peroxisomes as identified by the dark catalase reaction product were observed in two forms: (i) rounded to oval profiles and (ii) elongated, tubular, worm like structures, often bent, sometimes with a swollen end. Their sizes were also different. As measured manually the rounded profiles were 0·2–0·4 µm in diameter in the group situated at the apex and 0·4–0·7 µm for the basal organelles. The elongated forms were 0·1 µm thick and up to 1 µm, rarely 3 µm long. Some of the smaller rounded profiles must be cross sections of the elongated forms. But, in addition, a population of rounded or oval organelles, distinct from the tubular ones, must exist for the following reasons:

(1) Some of the rounded profiles have a greater small diameter than the elongated ones (Figs 3–7);

(2) Cells were encountered which show mainly or only rounded profiles, other cells showed a majority of elongated forms (Figs 3 and 4). If all rounded profiles were cross sections through elongated organelles, the latter must be orientated in a parallel array; but a longitudinal section of such a peculiar configuration was never observed. On the contrary, the elongated forms seemed to be orientated at random (Fig 3).

(3) Thick (0·4–1 µm) sections studied by electron microscopy showed the elongated forms to the best advantage (Fig 3). Larger rounded profiles were still recognised in such sections, however.

Morphometry confirmed the size difference (Table II). The frequency histogram of the formfactor (Fig 8) reflects profiles with widely divergent degrees of elongation. Subsequently, the lesser diameter (thickness) of the more rounded profiles with a formfactor between 1 and 0·65 was calculated separately from that of the elongated ones (formfactor below 0·65). The population with a high formfactor (rounded) (Fig 9) was found to contain: (i) many small profiles corresponding to cross sections of the elongated peroxisomes, and (ii) a tail to the right representing a few thicker organelles. The median width of the population within the tail but not present in the elongated group was 0·229–0·306 µm (see Table II). The population with the lower formfactor had a calculated lesser diameter of 0·090–0·116 µm (modus) (Fig 9).

TABLE II *Morphometry of duodenal peroxisomes*

Patient No	Age (years) /sex	No of peroxisomes	Volume density (%)	Surface density	Formfactor Maximum	Formfactor Minimum	Elongated (formfactor <0·65) Width (µm)	Elongated (formfactor <0·65) Area (10^{-3} µm²) Perimeter (10^{-3} µm)	Rounded (formfactor >0·65 or 0·80) Diameter (µm)	Rounded (formfactor >0·65 or 0·80) Area (10^{-3} µm²) Perimeter (10^{-3} µm)
1	59/M	892	0·990							
			0·613*	237*	0·909	0·161	0·096§	48·6	0·190§	18·3
			0·623†	240†			0·100‖	1123	0·229¶	512
			0·623‡	227‡						
2	19/M	296	0·731							
			0·483*	159*	0·899	0·322	0·116§	56·6	0·223§	25·6
			0·460†	152†			0·100‖	1208	0·236¶	619
			0·484‡	154‡						
3	60/F	592	0·773							
			0·486*	148*	0·914	0·288	0·107§	41·5	0·271§	36·2
			0·486†	148†			0·110‖	967	0·306¶	715
			0·541‡	153‡						
4	67/F	511	0·803							
			0·602*	178*	0·928	0·271	0·176§	43·6	0·300§	31·5
			0·490†	149†			0·090‖	979	0·426¶	670
			0·543‡	158‡						
5	79/F	216	0·676							
			0·450†	105†	0·915	0·240	0·115‖	46·1	0·274¶	44·8
			0·486‡	110‡				1017		810

*Corrected for cylinders, width measured manually.
†Corrected for cylinders using mode of calculated thickness of elongated forms (from Fig 9A).
‡Corrected for spheres the diameter of which is the mean D-circle of all rounded profiles – the diameter of the circle having the same area.
§Measured manually on calibrated electron micrographs.
‖Modus of calculated width (lesser diameter).
¶Median of calculated lesser diameter of the population of larger rounded profiles not present in the elongated group (tail of the histogram: see Fig 9B).

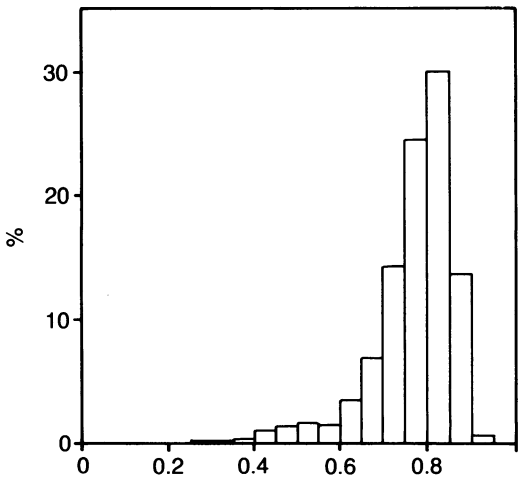

Figure 8: Frequency distribution of formfactor. Elongated organelles are at left, oval and more rounded profiles at right. After separating the groups at 0·65, their lesser diameter (width) was calculated (see Fig 9).

Although the tubular forms were thinner, their mean cross sectional area was equal or higher than it was in the rounded type (see Table II) – that is, due to their longest diameter they could contain more protein per organelle. The surface membrane of the elongated forms was also larger, as indicated by the perimeter of the profiles.

In patient 4 (Table II) morphometry showed a more complex situation. In addition to many slender, worm like forms (mode of lesser diameter: 0·90 μm), few shorter tubular profiles were seen, having a formfactor below 0·65 but a lesser diameter in the same range as the largest rounded profiles; both thickness-frequency histograms showed a tail to the right. So, in this duodenum evidence of truly spherical peroxisomes was limited to three organelles out of 590, which by manual measurement had a short diameter over 0·4 μm, a size not reached by tubular forms (maximum 0·28, 0·30, 0·37 μm). The duodenal mucosa was microscopically normal, but this patient had a gastric tumour.

Tubular peroxisomes were clearly distinct from cysternae of endoplasmic reticulum which were visible but negative for catalase reaction product (Figs 5 and 7). The degree of elongation differed between individuals, as was also confirmed by the minimum formfactor (Table II).

We also examined by tilting semithin sections whether overlapping tubular profiles were connected; when seen from a different angle, the tubules were not in contact.

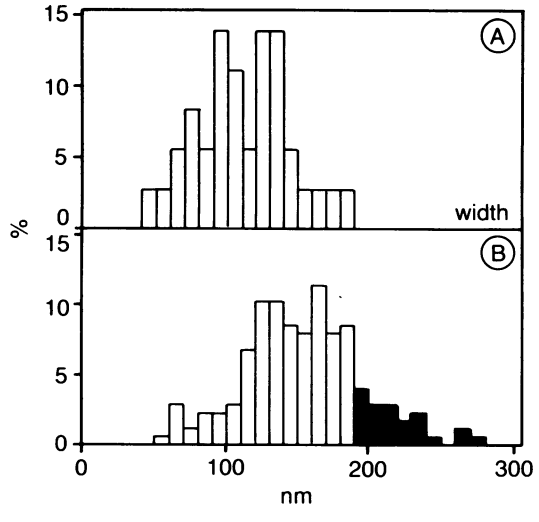

Figure 9: Frequency distributions of calculated width or lesser diameter of elongated (A) and rounded (B) profiles defined by their formfactor below 0·65 (A) or above (B). Rounded group B shows a tail to the right (black columns), representing organelles that are wider than the tubular forms. The median of these larger peroxisomes is given in Table II, after multiplying by 1·274 (see Methods). Patient 5.

In most patients a mixture of elongated and large rounded forms was found, often in the same epithelial cell (Fig 7). Predominantly rounded forms were found in one third, predominantly elongated ones in another third of the patients; but it cannot be excluded that a search in other blocks would have shown a different distribution.

Volume density was 0·68 to 0·99% without correction for section thickness. The corrected volume density remained an approximation because the correction factor is different for spheres and cylinders and an individual round profile cannot be identified as either of them. So, the modal diameter of true spheres is not known because they overlap with round profiles which are transverse sections of tubular peroxisomes. A correction factor for spheres was computed from the mean d-circle (diameter of circle with the same area) of the rounded profiles with a formfactor over 0·65; this obviously is an underestimation which leads to an underestimation of volume density. For cylinders two correction factors were obtained: (i) from the mode of the calculated lesser diameter and (ii) from the manually measured thickness in three individuals. No correction for truncation was carried out,[20] which underestimates volume density once more. Extreme values obtained for the corrected density were 0·45 and 0·62%. This compares with a mean (SEM) 1·05 (0·14)% in human liver.[21,22] Although no volume density figures are given by Black and Cornacchia,[16] a mean of 0·47% can be derived from their graph of control children.

The surface density of the peroxisomes – that is, the total area of their membrane, varied among individuals from 105 to $240 \cdot 10^{-3}$ μm^{-1}, the higher values corresponding to predominantly tubular populations (patients 1, 2, and 4). In four out of five duodenums surface density was significantly higher than it was in six control livers (mean (SEM) 105 (12)).

When the regional differences in the villus seen by light microscopy were studied ultrastructurally, peroxisomes were found at the villus tip, too; their number was equal or only slightly less than at the villus base or stem. At the tip staining often appeared weaker, and only elongated forms were present there, in contrast to the rounded forms at the base. The latter are larger, which should improve their visibility in the light microscope. In the crypts a few round and oval peroxisomes were seen in stem cells as well as in Paneth cells.

Discussion

Peroxisomes in human duodenal epithelium are divided by their formfactor and thickness into at least two populations: nearly spherical or oval organelles and tubular forms. The latter are thinner – that is, they have a lower small diameter but their area is equal or larger; they are distinct from the endoplasmic reticulum which is unreactive for catalase. Rounded and elongated forms were also described in fetal and neonatal

mice.[23 24] It was proposed[23] that the spherical type originates by budding from the elongated type, but according to Calvert and Menard[24] the rounded forms were seen first at 15 fetal days; the worm shaped ones only appeared several days later. In the guinea pig duodenum round and short elongated profiles were frequently found.[10] In one patient Novikoff *et al*[11] only showed round intestinal peroxisomes. Lazarow *et al*[15] reported round and elongated peroxisomes in a normal child. Black and Cornacchia[16] did not mention tubular forms in two control children but their Figure 3A shows a typical one.

Elongated peroxisomes are known in the normal human renal proximal tubule where they coexist with larger oval and triangular forms, not unlike what is seen in duodenal cells; in kidney, however, elongated profiles are much less frequently seen.[17] In contrast, normal hepatic peroxisomes are never tubular, and even in disease states such forms are very rare.[25 26] Our observations of the prevalence of rounded and tubular forms and their size difference do not suggest that one form has arisen from the other.

ROLE OF PEROXISOMES

Until recently, the role of duodenal peroxisomes was unknown.[27] We propose that they are important for fatty acid metabolism. Mucosa of the small intestine of guinea pig[28] and rat[29] possess peroxisomal acyl-CoA oxidase activity for β oxidation of fatty acids which is resistant to cyanide and forms hydrogen peroxide instead of H_2O. In hepatic peroxisomes this peroxide is broken down by catalase (experiment in the unanaesthetised animal).[30] In perfused small intestine or isolated epithelial cells oxygen consumption is largely insensitive to cyanide and azide; this is attributed to the peroxisomal fatty acyl-CoA oxidase.[31] Thomassen *et al*[29] showed chain shortening of intraluminally administered erucic acid (C-22) in the unanaesthetised rat. Overall fatty acid oxidation in the small intestine is increased during fasting, is accompanied by the liberation of glycerol, and proceeds without addition of substrate,[32] which indicates that endogenous triglycerides are being used.

It is likely that duodenal peroxisomes contribute appreciably to the normal breakdown of very long chain (C-22, C-24, C-26) fatty acids which are not metabolised by mitochondria. In human deficiency disorders of peroxisomal β oxidation, these fatty acids accumulate – for example, in the brain. Peroxisomal volume density in the duodenum, taking into account the underestimation of the corrected value, is not so much different from peroxisomal volume density in human liver. Although in rodents peroxisomal β oxidation capacity per gram of mucosa is 2·3 to 3·2 times less than in liver,[28 33] access of substrates and exchange of metabolites must be facilitated by the larger membrane area of elongated duodenal peroxisomes. It is remarkable that their surface density is 1·4 to 2·3 times higher than in liver (in four out of five people). In the living cell this may compensate for the lower enzymatic capacity as measured in homogenates. Data on β oxidation capacity in human duodenum are not available; catalase specific activity is a third to two thirds of that in human liver.[12 15]

Two more mechanisms favour intestinal metabolism of fatty acids compared with the liver: (i) an additional source of substrate: luminal fatty acids are oxidised for at least 17% and they provide 58% of the total oxidised fatty acids[34]; (ii) though in the liver peroxisomal β oxidation is lower in the fed state,[35] and is immediately inhibited by insulin or carbohydrate feeding,[30] in the small intestine fatty acids remain the major fuel of respiration in the presence of glucose utilisation.[32 36–38]

As in the liver the number and β oxidation capacity of intestinal peroxisomes are greatly enhanced by peroxisome proliferators such as clofibrate, at least in rodents.[29 33 39–41] β oxidation capacity may rise above the level in control liver.[33] A diet containing 43·5% of C-22 fatty acids induced peroxisomal β oxidation capacity in both the intestine and liver.[29] Phytanic acid, a branched fatty acid which accumulates in many peroxisomal disorders, also elicited peroxisomal proliferation in mouse duodenum, liver, and myocardium.[42]

At first sight, the gradient of peroxisomal catalase staining along the villus observed by light microscopy does not favour a relation between peroxisomal function and fat absorption, the latter being most active near the villus tip.[43] Ultrastructurally, however, peroxisomes are still present at the tip. Their lower catalase content probably reflects a normal turnover not compensated for by continuing synthesis when the cells grow older and move up the villus. Indeed, hepatic catalase has a half-life of only 1·5 days in the rat and 3·35 days in the guinea pig. Experimental inhibition of synthesis leads to smaller peroxisomes possessing only a fraction of their activity.[44] We propose that catalase synthesis takes place in the crypts and up to the mid-villus. Many enzymes, including those for fat metabolism, show a gradient along the villus axis.[34 45–48]

The important role of peroxisomes in intestinal function is further suggested by the drastic increase of these organelles after metamorphosis in two anuran species,[49] and by the impressive modulation of duodenal peroxisomes in rickets and vitamin D repletion.[50]

INHERITED DISORDERS

Lazarow *et al*[15] reported rare and small intestinal peroxisomes in two children with the cerebrohepatorenal syndrome of Zellweger. Black and Cornacchia[16] performed morphometry on these biopsy specimens and on one from a child with neonatal adrenoleucodystrophy. In the latter the peroxisomes were smaller but there were no fewer, than in two control children. Thus the behaviour of duodenal peroxisomes in these diseases differs from that in the liver: in the cerebrohepatorenal syndrome hepatic peroxisomes are not recognisable, and in the neonatal adrenoleucodystrophy syndrome they are very rare and small, representing 1% only of the normal volume density.[1] Black and Cornacchia[16] did not mention the existence in their control subjects of elongated peroxisomes, but in neonatal adrenoleucodystrophy they described long

tubular elements reacting for catalase activity; they considered these as precursors reflecting the defect in peroxisomal assembly, and compared them to the peroxisomal reticulum proposed by Lazarow *et al*[51] and Gorgas.[52 53] Our observations on thick sections and our tilting experiment do not confirm the existence of such a reticulum in enterocytes of normal adults.

If duodenal peroxisomes are active in the breakdown of very long chain fatty acids their presence in neonatal adrenoleucodystrophy raises the question of the mechanism of fatty acid accumulation present in this disease. Either the residual peroxisomal mass (1% in liver, 50% in the intestine) is insufficient or it is accompanied by an enzymatic deficiency. Localisation of β oxidation enzymes by immunocytochemistry[54] might shed more light on this question. In rectal mucosa Shimozawa *et al*[55] showed the deficiency of several β oxidation enzymes in biopsy specimens from three patients with Zellweger syndrome.

We are indebted to Dr A Cornelis for performing the tilting experiments, and to Professor G Devis (Department of Gastroenterology) for his support and encouragement. René Stien printed the photographs. For electron microscopy and morphometry equipment of the Department of Cell Biology and Histology (Professor E Wisse) was used. This investigation was supported by the Belgian FGWO 3.0071.83, 3.0034.86, and 3.0018.89, and by the Research Council of the Vrije Universiteit Brussel.

1 Goldfischer S, Collins J, Rapin I, Coltoff-Schiller B, Chang CH, Nigro M, *et al*. Peroxisomal defects in neonatal-onset and X-linked adrenoleukodystrophy. *Science* 1985; **227**: 67–70.
2 Schutgens RBH, Heymans HSA, Wanders RJA, Van den Bosch H, Tager JM. Peroxisomal disorders: a newly recognised group of genetic diseases. *Eur J Pediatr* 1986; **144**: 430–40.
3 Roels F, Cornelis A, Poll-The BT, Aubourg P, Ogier H, Scotto JM, *et al*. Hepatic peroxisomes are deficient in infantile Refsum disease. A cytochemical study of 4 cases. *Am J Med Genet* 1986; **25**: 257–71.
4 Heymans HSA, Oorthuys JWE, Nelck G, Wanders RJA, Dingemans KP, Schutgens RBH. Peroxisomal abnormalities in rhizomelic chondrodysplasia punctata. *J Inher Metab Dis* 1986; **9** (suppl 2): 329–31.
5 Kalter DC, Atherton DJ, Clayton PT. X-linked dominant Conradi-Huenermann syndrome presenting as congenital erythroderma. *J Am Acad Dermatol* 1989; **21**: 248–56.
6 Danpure CJ, Cooper PJ, Wise PJ, Jennings PR. An enzyme trafficking defect in two patients with primary hyperoxaluria type 1: peroxisomal alanine/glyoxylate aminotransferase rerouted to mitochondria. *J Cell Biol* 1989; **108**: 1345–52.
7 Wanders RJA, Heymans HSA, Schutgens RBH, Barth PG, van den Bosch H, Tager JM. Peroxisomal disorders in neurology. *J Neurol Sci* 1988; **88**: 1–39.
8 Lazarow PB, Moser HW. Disorders of peroxisome biogenesis. In: Scriver CR, Beaudet AL, Sly WS, Valle D, eds. *The metabolic basis of inherited disease*. 6th ed. New York: McGraw-Hill, 1989: 1479–509.
9 Connock M, Pover W. Catalase particles in the epithelial cells of the guinea-pig small intestine. *Histochem J* 1970; **2**: 371–80.
10 Novikoff PM, Novikoff AB. Peroxisomes in absorptive cells of mammalian small intestine. *J Cell Biol* 1972; **53**: 532–60.
11 Novikoff AB, Novikoff PM, Davis C, Quintana N. Studies on microperoxisomes. II. A cytochemical method for light and electron microscopy. *J Histochem Cytochem* 1972; **20**: 1006–23.
12 Peters TJ. Analytical subcellular fractionation of jejunal biopsy specimens; methodology and characterization of the organelles in normal tissue. *Clin Sci Mol Med* 1976; **51**: 557–74.
13 Roels F, Van der Spek P, Pauwels M. Peroxisomes in human duodenal epithelium visualized by catalase cytochemistry. *J Histochem Cytochem* 1983; **31**: 1065.
14 Van der Spek P, Espeel M, Cornelis A, Roels F. Peroxisomes (microbodies) in liver and duodenal biopsies. *Acta Endoscopica* 1985; **15**: 106–7.
15 Lazarow PB, Black V, Shio H, Fujiki Y, Hajra AK, Datta NS, *et al*. Zellweger syndrome: biochemical and morphological studies on two patients treated with clofibrate. *Pediatr Res* 1985; **19**: 1356–64.
16 Black VH, Cornacchia L III. Stereological analysis of peroxisomes and mitochondria in intestinal epithelium of patients with peroxisomal deficiency disorders: Zellweger's syndrome and neonatal-onset adrenoleukodystrophy. *Am J Anat* 1986; **177**: 107–18.
17 Roels F, Goldfischer S. Cytochemistry of human catalase. The demonstration of hepatic and renal peroxisomes by a high temperature procedure. *J Histochem Cytochem* 1979; **27**: 1471–7.
18 Roels F, Verdonck V, Pauwels M, De Catte L, Lissens W, Liebaers I, *et al*. Light microscopic visualization of peroxisomes and plasmalogens in first trimester chorionic villi. *Prenat Diagn* 1987; **7**: 525–30.
19 Roels F, Wisse E, De Prest B, van der Meulen J. Cytochemical discrimination between catalases and peroxidases using diaminobenzidine. *Histochemistry* 1975; **41**: 281–312.
20 Weibel ER, Paumgartner D. Integrated stereological and biochemical studies on hepatocytic membranes. *J Cell Biol* 1978; **77**: 584–97.
21 De Craemer D, Espeel M, Langendries M, Schutgens RBH, Hashimoto T, Roels F. Post-mortem visualization of peroxisomes in rat and in human liver tissue. *Histochem J* 1990; **22**: 36–44.
22 De Craemer D, Rickaert F, Wanders RJA, Roels F. Hepatic peroxisomes are smaller in primary hyperoxaluria type I (PH.I) Cytochemistry and morphometry. *Micron Microscopica Acta* 1989; **20**: 125–6.
23 Pipan N, Psenicnik M. The development of microperoxisomes in the cells of the proximal tubules of the kidney and epithelium of the small intestine during the embryonic development and postnatal period. *Histochemistry* 1975; **44**: 13–21.
24 Calvert R, Menard D. Cytochemical and biochemical studies on the differentiation of microperoxisomes in the small intestine of the fetal mouse. *Develop Biol* 1978; **65**: 342–52.
25 Roels F, Pauwels M, Poll-Thé BT, Scotto J, Ogier H, Aubourg P, *et al*. Hepatic peroxisomes in adrenoleukodystrophy and related syndromes: Cytochemical and morphometric data. *Virchows Arch* [A] 1988; **413**: 275–85.
26 Sternlieb I, Quintana N. The peroxisomes of human hepatocytes. *Lab Invest* 1977; **36**: 140–9.
27 Madara JL, Trier JS. Functional morphology of the mucosa of the small intestine. In: Johnson LR, ed. *Physiology of the gastrointestinal tract*. 2nd ed. New York: Raven Press, 1987: 1209–49.
28 Small GM, Brolly D, Connock MJ. Palmityl-CoA oxidase: detection in several guinea pig tissues and peroxisomal localization in mucosa of small intestine. *Life Sci* 1980; **27**: 1743–51.
29 Thomassen MS, Helgerud P, Norum KR. Chain-shortening of erucic acid and microperoxisomal β-oxidation in rat small intestine. *Biochem J* 1985; **255**: 301–6.
30 Van den Branden C, Kerckaert I, Roels F. Peroxisomal β-oxidation from endogenous substrates. Demonstration through H_2O_2 production in the unanaesthetized mouse. *Biochem J* 1984; **218**: 697–702.
31 Hülsmann WC. Energy metabolism in small intestine. In: Schiller CM, ed. *Intestinal toxicology*. New York: Raven Press, 1984: 57–67.
32 Lester RG, Grim E. Substrate utilization and oxygen consumption by canine jejunal mucosa in vitro. *Am J Physiol* 1975; **229**: 139–43.
33 Kawashima Y, Takegishi M, Watanuki H, Katoh H, Tachibana Y, Kozuka H. Effect of clofibric acid and tiadenol on peroxisomal β-oxidation and fatty acid binding protein in intestinal mucosa of rats. *Toxicol Appl Pharmacol* 1985; **78**: 363–9.
34 Gangl A, Ockner RK. Intestinal metabolism of plasma free fatty acids. Intracellular compartmentation and mechanisms of control. *J Clin Invest* 1975; **55**: 803–13.
35 Van den Branden C, Roels F. Thioridazine: a selective inhibitor of peroxisomal β-oxidation in vivo. *FEBS Lett* 1985; **187**: 331–3.
36 Hülsmann WC. Preferential oxidation of fatty acids by rat small intestine. *FEBS Lett* 1971; **17**: 35–8.
37 Frizzell RA, Markscheid-Kaspi L, Schultz SG. Oxidative metabolism of rabbit ileal mucosa. *Am J Physiol* 1974; **226**: 1142–8.
38 Lang CH, Alteveer RJ. Effects of glucose-insulin-potassium on intestinal hemodynamics and substrate utilization during endotoxemia. *Am J Physiol* 1986; **251**: G341–8.
39 Svoboda DJ. Response of microperoxisomes in rat small intestinal mucosa to CPIB, a hypolipidemic drug. *Biochem Pharmacol* 1976; **25**: 2750–2.
40 Psenicnik M, Pipan N. Nafenopin-induced proliferation of peroxisomes in the small intestine of mice. *Virchows Arch* [B] 1977; **25**: 161–9.
41 Calvert R, Malka D, Menard D. Effect of clofibrate on the small intestine of fetal mice. *Histochemistry* 1979; **63**: 7–14.
42 Van den Branden C, Vamecq J, Wybo I, Roels F. Phytol and peroxisomal proliferation. *Pediatr Res* 1986; **20**: 411–5.
43 Friedman HI, Nylund B. Intestinal fat digestion, absorption, and transport. A review. *Am J Clin Nutr* 1980; **33**: 1108–39.
44 Geerts A, De Prest B, Roels F. On the topology of catalase biosynthesis and degradation in the guinea pig liver. A cytochemical study. *Histochemistry* 1984; **80**: 339–45.
45 Padykula HA, Strauss EW, Ladman AJ, Gardner FH. A morphologic and histochemical analysis of the human jejunal epithelium in nontropical sprue. *Gastroenterology* 1961; **40**: 735–65.
46 Fortin-Magana R, Hurwitz R, Herbst JJ, Kretchmer N. Intestinal enzymes: Indicators of proliferation and differentiation in the jejunum. *Science* 1970; **167**: 1627–8.
47 Koster ASJ, Borm PJA, Dohmen MR, Noordhoek J. Localization of biotransformational enzymes along the crypt-villus axis of the rat intestine. Evaluation of two cell isolation procedures. *Cell Biochem Funct* 1984; **2**: 95–101.
48 Hülsmann WC, Kurpershoek-Davidov R. Topographic distribution of enzymes involved in glycerolipid synthesis in rat small intestinal epithelium. *Biochim Biophys Acta* 1976; **450**: 288–300.

49 Dauca M, Calvert R, Menard D, Hugon JS, Hourdry J. Development of peroxisomes in amphibians. I. Cytochemical and biochemical studies on the small intestine. *J Exp Zool* 1982; **220**: 235–41.

50 Davis WL, Jones RG. Peroxisomes in the absorptive cells of normal, rachitic, and vitamin-D replete chick intestine: ultrastructure and histochemistry. *Tissue Cell* 1984; **16**: 443–53.

51 Lazarow PB, Robbi M, Fujiki AK, Wong L. Biogenesis of peroxisomal proteins in vivo and in vitro. *Ann NY Acad Sci* 1982; **386**: 285–98.

52 Gorgas K. Peroxisomes in sebaceous glands. 5. Complex peroxisomes in the mouse preputial gland: serial sectioning and three-dimensional reconstruction studies. *Anat Embryol (Berl)* 1984; **169**: 261–70.

53 Gorgas K. Serial section analysis of mouse hepatic peroxisomes. *Anat Embryol (Berl)* 1985; **172**: 21–32.

54 Espeel M, Hashimoto T, De Craemer D, Roels F. Immunocytochemical detection of peroxisomal β-oxidation enzymes in cryostat and paraffin sections of human post mortem liver. *Histochem J* 1990; **22**: 57–62.

55 Shimozawa N, Suzuki Y, Orii T, Yokota S, Hashimoto T. Biochemical and morphologic aspects of peroxisomes in the human rectal mucosa: diagnosis of Zellweger syndrome simplified by rectal biopsy. *Pediatr Res* 1988; **24**: 723–7.